Translational Oncology 25 (2022) 101507

Contents lists available at ScienceDirect

Translational Oncology

journal homepage: www.elsevier.com/locate/tranon

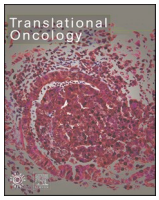

Low levels of miR-34c in nasal washings as a candidate marker of aggressive disease in wood and leather exposed workers with sinonasal intestinal-type adenocarcinomas (ITACs)

Elisabetta Bigagli [a], Giandomenico Maggiore [b], Lorenzo Cinci [c], Mario D'Ambrosio [a], Luca Giovanni Locatello [b,*], Cosimo Nardi [c], Annarita Palomba [d], Gianluca Leopardi [e], Pietro Orlando [b], Giuseppe Licci [b], Oreste Gallo [b], Cristina Luceri [a,*]

[a] Department of Neuroscience, Psychology, Drug Research and Child Health (NEUROFARBA) Section of Pharmacology and Toxicology, University of Florence, Florence, Italy
[b] Department of Otorhinolaryngology, Careggi University Hospital, University of Florence, Florence, Italy
[c] Department of Experimental and Clinical Biomedical Sciences, Radiodiagnostic Unit n. 2, Careggi University Hospital, Florence, Italy
[d] Section of Pathological Anatomy, Department of Health Sciences, Azienda Ospedaliero-Universitaria Careggi, University of Florence, Italy
[e] Ospedale S. Giuseppe Empoli

ARTICLE INFO

Keywords:
Intestinal-type sinonasal adenocarcinomas
ITAC
MicroRNA
Noncoding RNA
Biomarkers

ABSTRACT

Introduction: Sinonasal intestinal-type adenocarcinomas (ITACs) are rare and aggressive tumors, closely related to professional exposure to wood dusts or leather. Here we explored the role of non-coding RNAs controlling MUC2 in liquid biopsies and tumors from ITAC patients with the aim of identifying biomarkers and molecular mechanisms to improve early diagnosis, prognosis, and therapeutic approaches for this rare cancer.
Methods: MiR-34c-3p, lncRNA AF147447 and *MUC2* were measured in tumors and normal mucosa, in nasal washings (NW) from the affected and non-affected nostril and in plasma from 17 ITAC patients. The Apparent Diffusion Coefficient (ADC) was also evaluated by Magnetic Resonance Imaging.
Results: MiR-34c was higher in ITACs compared to the corresponding normal mucosa ($p = 0.021$). Differentiated tumors exhibited higher miR-34c levels ($p = 0.025$) and lower ADC values ($p<0.001$) compared to mucinous ones and these parameters were also inversely correlated ($r = 0.87$; $p = 0.001$). High *MUC2* tumor expression was associated with orbital extension ($p = 0.010$). Low miR-34c levels in NW were associated with orbital ($p = 0.009$) and intracranial ($p = 0.031$) extension and with advanced TNM stage ($p = 0.054$). Functional analysis identified Wnt, Focal adhesion, MAPK and inflammatory signalings among the pathways most enriched in mir-34c targets.
Discussion: Our results suggest measuring miR-34c in NW as a biomarker for early diagnosis and monitoring of ITAC patients and for the surveillance of wood and leather exposed workers. Further research on the involvement of miR-34c regulated pathways in ITAC tumorigenesis may also allow the development of new therapeutic approaches for this rare cancer.

Introduction

Sinonasal intestinal-type adenocarcinomas (ITACs) are rare tumors etiologically related to professional exposure to wood dusts or leather [1,2]. Owing to nonspecific symptoms, these tumors are often diagnosed at an advanced stage (III-IV) when already invading critical surrounding tissues such as the orbit and brain [3]. ITAC patients have an unfavorable prognosis, with a five-year survival rate dropping from 80% for stage I to 35% for stage IV tumors [4]. Local recurrences often occur and represent the main cause of death even after radical surgery and adjuvant radiotherapy, while chemotherapy yields unsatisfactory results [5,6].

The identification of early diagnostic biomarkers and novel molecular mechanisms underlying ITAC tumorigenesis is expected to improve the prognosis and the therapeutic approaches for this disease. Accumulating evidence suggests that circulating tumor cells, cell-free DNA,

* Corresponding authors.
E-mail addresses: locatello.lucagiovanni@gmail.com (L.G. Locatello), cristina.luceri@unifi.it (C. Luceri).

https://doi.org/10.1016/j.tranon.2022.101507
Received 21 April 2022; Received in revised form 26 July 2022; Accepted 28 July 2022

and non-coding RNAs (including long noncoding RNA (lncRNA) and microRNAs (miRNAs)), might be promising biomarkers in the early diagnosis and prognosis of cancer [7–12]. Thanks to their ability to concurrently target multiple genes involved in tumor development and progression, miRNA-based treatments, either as drugs or as drug targets, alone or in combination with chemotherapy and/or radiotherapy, showed promise to improve treatment strategies in some cancers [13, 14].

Only two studies evaluated miRNAs expression in ITACs: reduced tissue and plasma miR-126 expression was reported in ITAC patients compared to controls, while miR-205 and miR-449a/ miR-34c cluster were associated with a worse prognosis [15,16].

MiR-34c is often down-regulated in cancers playing a tumor-suppressive role through the regulation of genes involved in proliferation, survival, apoptosis, cell growth, invasion, and metastasis [17]. In addition, Zhou et al. [18] demonstrated that miR-34c and lncRNA AF147447 inhibited gastric cancer proliferation and invasion by targeting Mucin 2 (MUC2), a gel-forming glycoprotein prevalently expressed in mucinous ITACs and associated with distant metastasis [19].

The analysis of circulating and tumor levels of miR-34c and lncRNA AF147447 in ITAC may support their possible application as biomarkers, the identification of pathways of disease development and progression and the discovery of potential novel targets and therapeutic approaches.

With this aim, we investigated the expression of miR-34c, lncRNA AF147447 and *MUC2* mRNA in tissues, plasma, and nasal washings from ITAC patients and their associations with clinicopathological and Magnetic Resonance Imaging (MRI) characteristics.

Methods

Patients and samples collection

This prospective study was approved by the local Institutional Review Board (Comitato Etico Area Vasta Centro, ref. 196,237/oss). In the period 2019–2021, a total of seventeen patients with histologically proven sinonasal ITACs were recruited at the Department of Otorhinolaryngology, Careggi University Hospital, Florence, after signing the written informed consent. In two cases of inoperable disease, no extensive tumor sampling was possible and only nasal washings (NW) and plasma were collected.

Fifteen sample pairs (from the primary ITAC mass, along with the contra-lateral non-tumor sinonasal mucosal tissue) were collected from patients during endoscopic oncological surgery and stored at − 20 °C.

Nasal washings were instead collected the day of surgery or the day of in-office diagnosis, for inoperable patients. Nasal washings were collected both from the sinonasal cavity affected and form the contralateral one as follows: in the sitting position after cleaning the skin of the nose with alcoholic solution, the tube adapter for the mask version of Rhinomanometry for ZAN 100 (Rhino Flow Handy II, ZAN, Messgeraete Gmbh, Germany), was fixed to each nostril. A syringe with 10 ml of physiological solution was connected to the device and the patient's head was flexed about 30° forward. After a high flow washing with saline solution, the material present in the nasal cavity was withdrawn with the same syringe and placed in a test tube. All samples were immediately stored at −20 °C.

Blood samples (5 mL) were collected on EDTA vacutainer, centrifuged at 2000 rpm for 10 min to separate the plasma. Plasma was then aliquoted and stored at − 20 °C for further analyses.

RNA extraction, miRNA and lncRNA analysis

Total RNA was isolated from plasma, nasal washings and tissues using the TRIzol Reagent (Invitrogen) according to the manufacturer's instructions. RNA was quantified by using the NanoPhotometer® (Implen, Munich, Germany) measuring the absorbance at 260 nm. cDNA was synthesized using the miRCURY LNA RT kit (Qiagen, Hilden, Germany). Reverse-transcription (RT) reaction was performed as follows: 2 μL miRCURY RT Reaction Buffer, 4.5 μL RNase-free water, 1 μL miRCURY RT Enzyme Mix, 0.5 μL UniSp6 spike-in, and 2 μL template RNA (5 ng/μL). RT cycling protocol consisted in 60 min at 42 °C, 5 min at 95 °C, and cooling at 4 °C. cDNA samples were stored at −20 °C. RT-quantitative PCR (qPCR) was performed using miRCURY LNA SYBR Green PCR kit (Qiagen) and primers from miRCURY LNA miRNA PCR Assays (mir-34c-3p: cat. n. YP00204373, Qiagen; RNU6b: cat. n. YP00203907, Qiagen).) cDNA was diluted at the ratio of 1:30 for plasma and of 1:60 for tumor specimens and nasal washings. The analyses were performed using the Rotor-Gene Q thermal cycler (Qiagen). Cycling program consisted in 2 min at 95 °C and 2- step cycling (40 cycles) of denaturation (10 s at 95 °C), and combined annealing/extension (60 s at 56 °C). Each sample was tested in triplicate. RNU6b was selected as reference miRNA due to its stability across samples. The calculation of relative expression was performed using $2^{-\Delta\Delta Ct}$ for nasal washings and tissue samples and $2^{-\Delta Ct}$ for plasma and expressed as log2.

For lncRNA AF147447 and *MUC2* mRNA analyses, total RNA (500 ng) was reverse transcribed by using the RevertAid RT Kit (Thermo Scientific, Waltham, MA, USA); RT reaction was performed as follows: 4 μL 5X Reaction Buffer, 2 μL dNTPs Mix, 1 μL Random Hexamer Primer (N6), 1 μL RevertAid Reverse Transcriptase,1 μL RiboLock RNase Inhibitor, 10 μL RNA, 1 μL RNase-free water. RT cycling protocol consisted in 60 min at 45 °C, 5 min at 70 °C and cooling at 4 °C. cDNA samples were stored at −20 °C. RT performed using the Gene Amp 9700 (Applied Biosystem, Waltham, MA, USA) cycler.

RT-quantitative PCR (qPCR) was performed using the SsoAdvanced Universal SYBR (Biorad, Milan, Italy) as follows: 5 μl 2x SsoAdvanced Universal SYBR Green Supermix, 1 μl Primer forward, 1 μl Primer reverse, 1 μl cDNA, 2 μl RNase-free water. cDNA was diluted at the ratio of 1: 10. The primer sequences are as follows: lncRNA AF147447: forward 5′-TCCTCTAATGCGTCTTGTCTCC-3′, reverse 5′-CCCATACCAAACTCTAACCACC-3′; *MUC2*: forward 5′-GAGGTGGAGCGGGACAA-3′, reverse 5′-GCAGGGTGCTTTCGGC-3′; *GAPDH*: forward 5′-TGTGTTGGCGTACAGGTCTTTG-3′, reverse 5′-GGGAAATCGTGCGTGACATTAAG-3′). Cycling program consisted in incubation for 30 s at 95 °C and 2- step cycling of denaturation (15 s at 95 °C) and combined annealing/extension (15 s at 60 °C) for 35 cycles. The analyses were performed using the Rotor-Gene Q thermal cycler (Qiagen). Each sample was tested in triplicate. *GAPDH* was selected as reference miRNA due to its stability across samples. The calculation of relative expression was performed using $2^{-\Delta\Delta Ct}$ and expressed as log2.

MUC2 immunohistochemistry and clinico-pathological classification

Immunohistochemistry for MUC2 was carried out on histological sections, 5 μm thick, of formalin-fixed, paraffin-embedded ITAC samples provided by the Pathological unit. Sections were rehydrated, treated with citrate buffer at 90 °C for 1 h to retrieve antigen, then with 0.3% (v/v) H2O2 in 60% (v/v) methanol to quench endogenous peroxidase. Aspecific sites saturation was carried out by incubation at room temperature for 15 min with 1% BSA and 0.1% TRITON X in PBS. The specimens were then incubated overnight with rabbit polyclonal anti-MUC2 antibody at final dilution of 1:50 (sc-15,334 Santa Cruz Biotech). Immuno reaction was revealed by biotinylated anti-rabbit secondary antibody at final dilution of 1:200 and then by immunoperoxidase method (Vectastain Elite kit, Vector, Burlingame, CA, USA), using 3,3′-diaminobenzidine as chromogen. As negative controls, sections incubated with only the primary or the secondary antisera were used. Positivity for MUC2 immunoreaction was carried out by two independent observers in blind fashion by using a Reichert–Jung Microstar IV light microscope (Cambridge Instruments, Buffalo, NY, USA) at ×200 final magnification (test area: 72 346 μm2).

AJCC VIII Edition TNM classification was used for clinical staging [20], while all ITAC cases were reviewed by an expert head and neck

pathologist and Barnes's classification was implemented for defining each subtype [21].

miR-34c-3p gene target prediction and pathway functional analysis

Putative miR-34c-3p targets were predicted using miRTarBase database that provides information on experimentally validated miRNA-target interactions or by using Target Scan (https://www.targetscan.org/vert_80/) [22]. Pathway analysis was then performed in order to generate hypotheses about the relevant biological functions controlled by the miR-34c-3p-target interactions by using the GO-Elite pathway analysis tool (freely available at http://www.genmapp.org/go_elite/) and the list of target genes as input file.

Magnetic resonance imaging (MRI)

MRI were assessed in a subset of patients ($n = 10$) in which the pre-surgical MRI was carried out at the Careggi University Hospital, Florence, Italy. MRI scans in ITAC patients were performed via 1.5 T Magnetom Aera (Siemens Healthcare, Erlangen, Germany) with a devoted head and neck coil. The MR acquisition protocol (Supplementary Table 1) included an axial fat saturated echo-planar imaging-based Diffusion Weighted Imaging (DWI) with two different b-values (b 50–800 s/mm2). Apparent Diffusion Coefficient (ADC) maps were reconstructed from DWI images. ADC values were calculated by positioning three regions of interest (ROI) with an average intratumoral area of 0.30–0.40 cm2 each on three contiguous axial sections. ADC value of the trapezius muscle on the same side of the tumor were also obtained and ADC ratio was calculated as ADC_{ITAC}/ADC_{muscle}. ADC values were obtained by two independent observers in a blinded fashion.

DWI is a MR imaging technique based upon measuring the random Brownian motion of water molecules within a voxel of tissue. The extent of tissue cellularity and/or high cellular crowding determine the impedance of water molecule diffusion that can be quantitatively assessed using ADC values, displayed as a parametric map reflecting the degree of diffusion of water molecules through different tissues.

Statistical analysis

Categorical variables were described using proportions and compared by Fisher's exact test. Continuous data, including ADC values, were expressed as mean ± SD, or median value and interquartile range (IQR), and compared by Student's t-test or by Mann–Whitney U test, as requested by data distribution. Wilcoxon matched-pairs signed-ranks test was used to compare the expression of mir-34c, lncRNA AF147447 and *MUC2* mRNA in tumoral tissue vs. normal mucosa. The correlation between ADC ratio and miR-34c and between mir-34c and lncRNA AF147447 in plasma samples was assessed by linear regression analysis. A $p<0.05$ was considered statistically significant. Statistical analysis was performed using GraphPad Prism 8.0 (GraphPad Software, Inc., La Jolla, CA, USA).

Results

Characteristics of ITAC patients

The main clinicopathological features of ITAC patients are summarized in Table 1. All patients were males, 9 smokers and 8 never-smokers, with a mean age of 73.5 years, and all were professionally exposed to wood (53%) or leather (47%). The mean latency period from the last known exposure and ITAC diagnosis was 32.3 (range 20–41) years. At the time of diagnosis, three patients had already distant metastases, while no nodal metastases were present. Overall, we had stage II-III (41%), stage IVA/B (41%), stage IVC (18%) cases. The distribution by histological subtype was as follows: 7 patients (41%) had a mucinous subtype, 4 patient (24%) had a well differentiated tumor, and 6 patients (35%) had a moderately or poorly differentiated tumor. Orbital extension was documented in 6 (35%) and intracranial extension in 8 (47%) patients. Within a median time of 27 months, 3 patients died of the disease, and none was lost at follow-up.

Table 1
Overview of the clinical and pathological characteristics of ITAC patients.

N	17
Age, mean±SE	73.47±2.4
Sex, male	17 (100%)
Smokers	
No	8 (47%)
Yes	9 (53%)
Professional exposure	
wood	9 (53%)
leather	8 (47%)
Histotype	
mucinous	7 (41%)
well differentiated	4 (24%)
moderately-poorly differentiated	6 (35%)
TNM	
II-III	7 (41%)
IV A-B	7 (41%)
IVC	3 (18%)
Orbital extension	
no	11 (65%)
yes	6 (35%)
Intracranial extension	
no	9 (53%)
yes	8 (47%)
Survival	
alive	14 (82%)
died of disease	3 (18%)

Mir-34c, lncRNA AF147447 and MUC2 mRNA expression in paired samples of tumor tissue and normal mucosa

Higher tumor expression of miR-34c was found when we compared ITAC tissues to their respective paired normal mucosae, independently of histological subtypes (Fig. 1, panel A; $p = 0.0215$). However, when different subtypes were analyzed separately and compared to their paired normal mucosae, miR-34c was overexpressed only in differentiated tumors and not in the mucinous ones (Fig. 1, panel B; $p = 0.0039$). In addition, miR-34c was significantly lower in tumor tissue from mucinous ITACs compared to differentiated ones ($p = 0.0256$).

No differences in the expression of lncRNA AF147447 or *MUC2* mRNA in paired samples of tumor tissue and normal mucosa were observed (Fig. 1, panel C and D). Immunohistochemical positivity for MUC2 was detected in 30.76% of our cases: in 40% of mucinous tumors and in 25% on non-mucinous ITACs.

Mir-34c and MUC2 expression in ITAC tissues: correlation with pathological features

Although not statistically significant, when miR-34c tumor expression was dichotomized according to the median value of the group, high tumor levels of miR-34c were associated to lower stage: 62% of patients with TNM II-III and no patient with stage IVC had high miR-34c tumor expression (Fig. 2, panel A; $p = 0.11$). *MUC2* mRNA expression in tumor specimens was significantly associated with orbital extension ($p = 0.0103$) (Fig. 2, panel B).

Mir-34c and lncRNA AF147447 expression in the plasma and in paired samples of nasal washings from ITAC and from the unaffected sinonasal cavity

Both mir-34c and lncRNA AF147447 were detectable in the plasma and nasal washings from ITAC patients. In nasal washings, mir-34c was

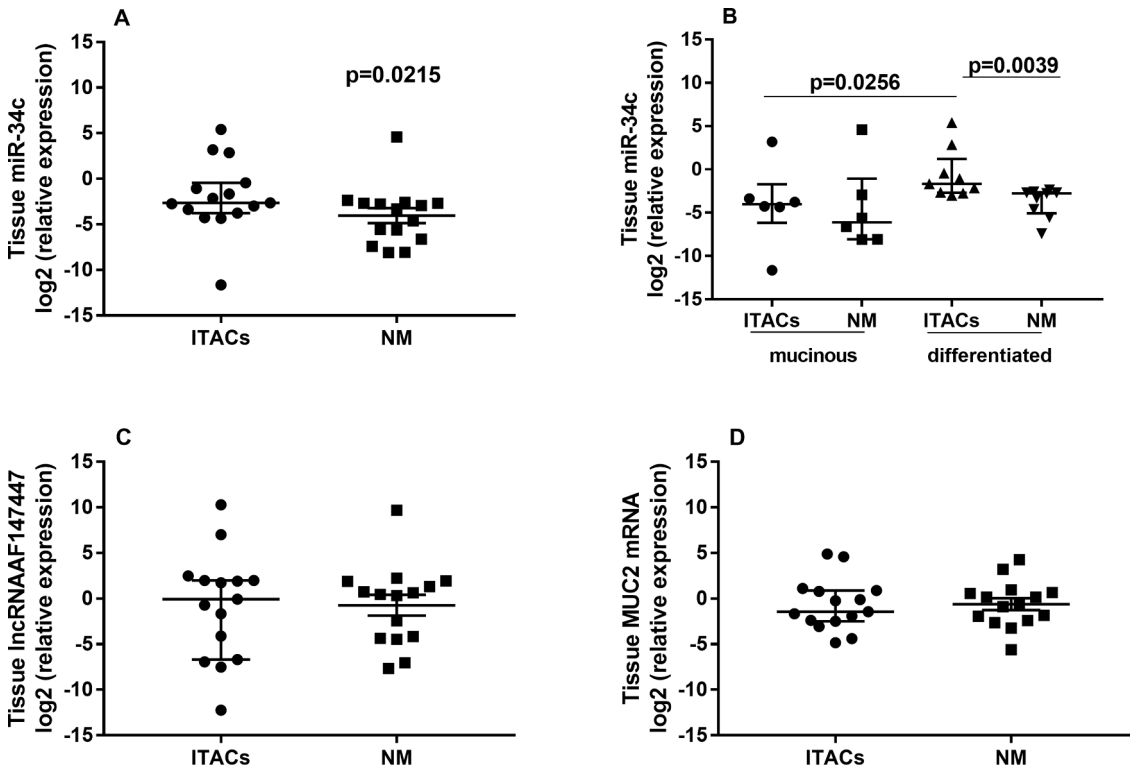

Fig. 1. Expression of Mir-34c in sample pairs of tumors and normal mucosae of ITAC patients (panel A) and in tumors and normal mucosae of ITAC patients according to their histological subtype (panel B). Expression of lncRNA AF147447 (panel C) and *MUC2* mRNA (panel D) in sample pairs of tumors and normal mucosae of ITAC patients. The horizontal marks indicate the median values and interquartile ranges.

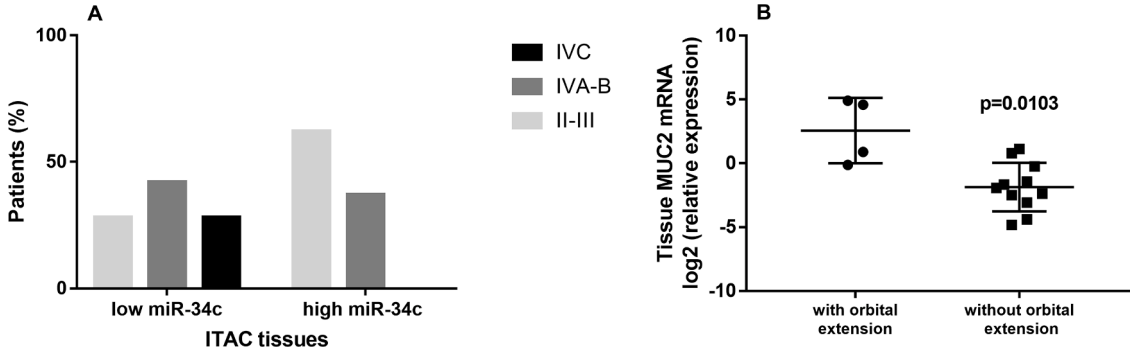

Fig. 2. Percentage of ITAC patients with IVC, IVA-B or II-III TNM stage, according to miR-34c expression in tumor tissues (panel A). *MUC2* mRNA expression in tumor specimens from patients with and without orbital extension (panel B). The horizontal mark indicates the mean±SD.

more abundant than lncRNA AF147447 but both showed similar levels in samples collected from the affected and from the non-affected sinonasal cavity (data not shown). In plasma samples, on the contrary, the lncRNA AF147447 was more abundant. A borderline significant decrease in miR-34c plasma levels in patients with TNM stage IV compared to those with stage II-III ($p = 0.0721$) was also observed (Supplementary Fig. 1). Linear regression showed that mir-34c and lncRNA AF147447 plasma levels were positively correlated ($r = 0.7483$; $p = 0.005$), (Supplementary Fig. 2).

Mir-34c and lncRNA AF147447 expression in nasal washings: correlations with clinicopathological features of ITAC patients

Low expression of miR-34c in nasal washings was significantly associated with both orbital and intracranial extension ($p = 0.009$ and $p = 0.0315$, respectively; Fig. 3, panel A and B). A borderline association with advanced TNM stage and low expression of miR-34c in nasal washings was also found ($p = 0.054$) while high levels of lncRNA AF147447 were significantly associated to orbital extension ($p = 0.0071$) (Fig. 3, panel C and D). Within our follow-up period, three deaths were registered, all patients displaying miR-34c nasal washings levels below the median level; however, this association was not statistically significant ($p = 0.25$) (Supplementary Fig. 3**)**.

The horizontal mark indicates the mean±SD.

Magnetic resonance imaging of ITAC tissue and correlations with mir-34c

A significant inverse correlation between ADC ratio and miR-34c expression in ITAC tissue was observed ($r = 0.87$; $p<0.05$) (Fig. 4, panel A). Moreover, patients with differentiated ITAC subtypes showed an ADC ratio (ADC ITAC/ADC muscle) significantly lower than those with mucinous ones (Fig. 4, panel B).

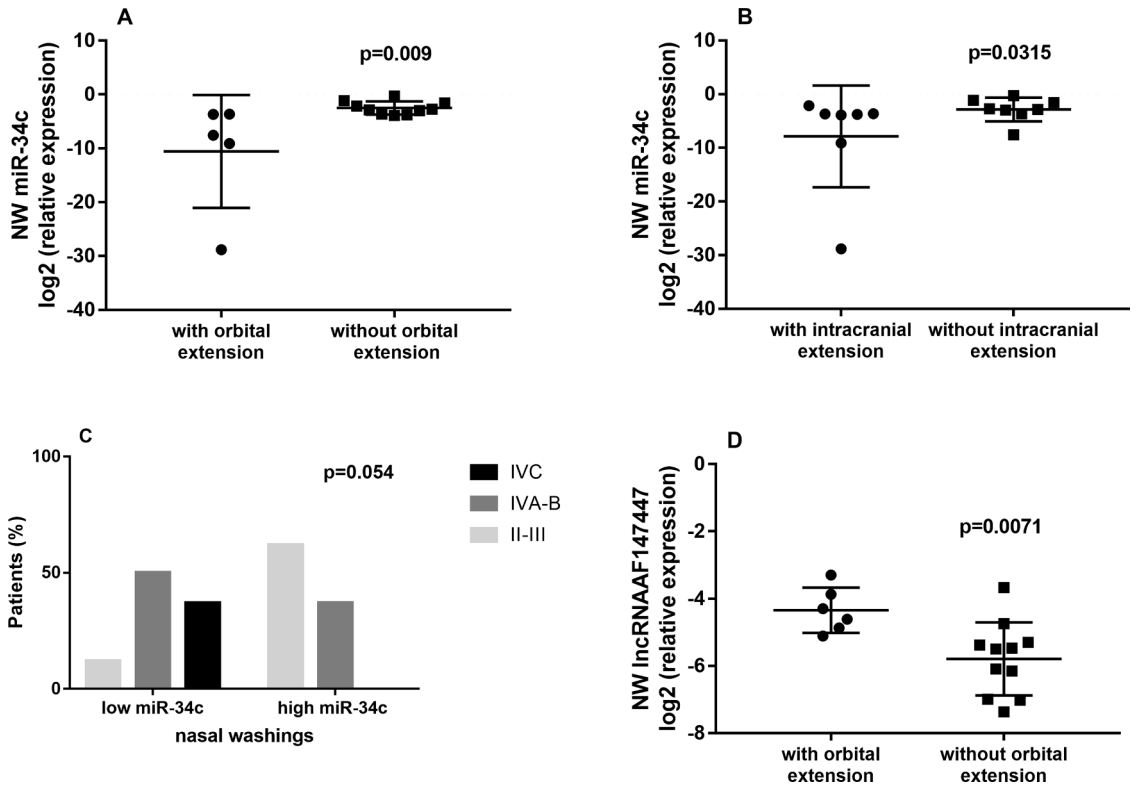

Fig. 3. Expression of Mir-34c in nasal washings (NW) from patients with and without orbital extension (panel A) and with and without intracranial extension (panel B). Percentage of ITAC patients with IVC, IVA-B or II-III TNM stage, according to miR-34c expression in NW (panel C). Expression of lncRNA AF147447 in NW from patients with and without orbital extension (panel D).

Target gene prediction of miR-34c and functional analysis

To elucidate the biological functions and signaling pathways associated with miR-34c, target gene prediction was performed using mirTarBase algorithm and a total of 1386 genes were identified (accessed on March 10, 2022). These target genes are enriched in 6 KEGG and 13 Wiki pathways linked to tumorigenesis and inflammation (Wnt, Focal adhesion and MAPK pathway, mTOR, phagocytosis, IL-1, T-Cell Receptor and Co-stimulatory Signaling and Interferon type I) as shown in Table 2.

Discussion

Several studies demonstrated that miRNAs are involved in the development and progression of head and neck cancers either behaving as tumor-promoting miRNAs (oncomiRNAs) or as tumor suppressor miRNAs [11, 12], but so far, only two studies addressed their relevance in ITACs [15,16].

MiR-34c is a recognized tumor suppressor able to inhibit cell migration and invasion *in vitro* and to prevent tumor growth and metastasis in an *in vivo* xenograft model of nasopharyngeal carcinoma [23]. Accordingly, mir-34c is down regulated in nasopharyngeal, laryngeal and lung cancers [24–29]. In addition, low mir-34c expression correlates with worse disease-free and overall survival in laryngeal and lung cancer patients [30–32] and with radioresistance [29].

Re et al. (2021) reported no differences in the expression of miR-34c in ITAC samples compared to adjacent normal mucosa but high miR-34c tumor expression correlated with poor disease-free and overall survival [16].

Our results add new translational insights on the clinical and biological significance of mir-34c in ITAC patients since its expression varies across different subtypes, being downregulated in mucinous ITAC compared to differentiated tumors. Since the mucinous subtypes carry a poor prognosis [33], it can be hypothesized that the downregulation of mir-34c may contribute to tumor aggressiveness. This is consistent with the tumor suppressive role of mir-34c against cancer cell growth, invasion, and metastasis by targeting Notch2, c-Met-and CDK1 [24,27,32].

MRI is part of the ITAC diagnostic workup and a miRNA–MRI integrated analysis has been proposed as an innovative tool in prostate tumors [34], but has never been explored in ITAC. As previously reported in mucinous lung cancers [35], our mucinous ITAC cases had higher ADC values than differentiated carcinomas likely because mucinous subtypes present lower cellular crowding and mucous content; moreover, ours is the first study to report an inverse correlation between miR-34c and ADC values in ITAC; despite being a preliminary finding that warrants further validations, it suggests that ADC values may vary according to tumor molecular features; accordingly, radiogenomic studies performed in breast, prostate, and ovarian cancers, demonstrated that ADC values may vary according to gene and receptor expression and p53 mutational status [36–38]; on this basis, a multidisciplinary approach integrating radiological findings with gene and miRNA expression holds promise to impact the characterization of these rare cancers.

Our group previously reported that the frequency of immunopositivity for MUC2 was higher in mucinous than non-mucinous subtypes [19] and the results of the present study confirm these findings. A functional link among MUC2, mir-34c and lncRNA AF147447 was reported in gastric cancer where lncRNA AF147447 repressed MUC2 expression by increasing miR-34c [18]; the lack of correlations among these biomarkers in ITAC tissues, suggests that these interactions have a marginal biological role in ITAC tumorigenesis and that other signalings, are likely involved. Accordingly, our functional analysis showed that miR-34c targets are associated with critical cancer pathways (e.g. focal adhesion, MAPK, Wnt, and mTOR) and with inflammatory signalings (e.g. phagocytosis, IL1, Interferon 1 and T cell receptor signaling). Wnt and MAPK have been reported among the most frequently mutated pathways in ITAC [39,40] and Wnt activation has been associated with worse

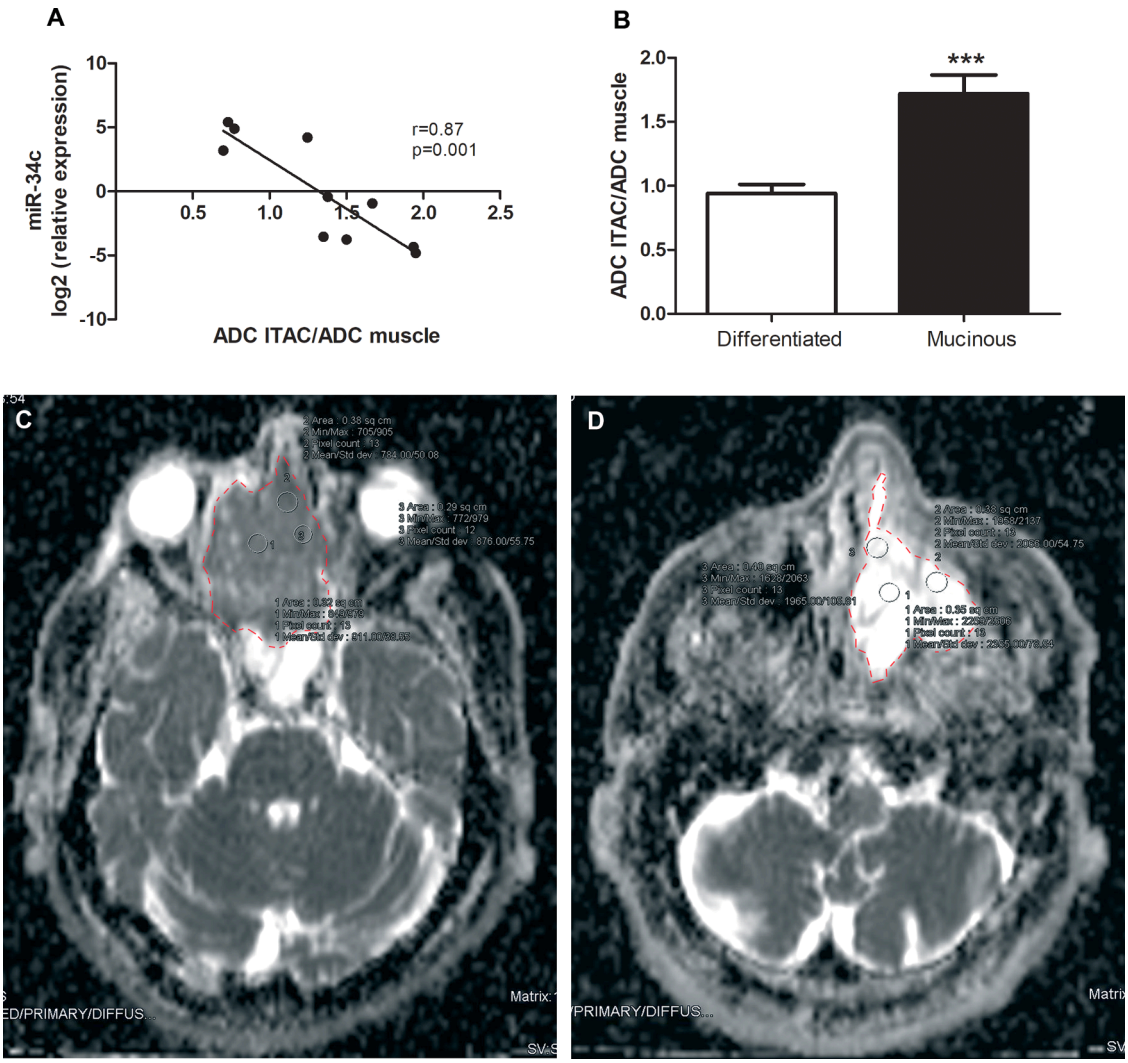

Fig. 4. MRI of ITAC tissue: correlations with mir-34c and histological subtypes. ADC values were expressed as the ratio between ADC of ITAC tissue and ADC of trapezius muscle on the same side. Panel A: correlation between ADC ratio and miR-34c expression in tumor samples; panel B: ADC ratio in differentiated and mucinous ITAC histological subtypes. *** $p<0.001$. Axial ADC representative images: panel C) ITAC with low ADC ratio; panel D) ITAC with high ADC ratio. ITAC tumours are highlighted with red dashed lines and three exemplificative ROIs for each ITAC are reported.

prognosis in these patients [41]. The role of inflammation in ITAC is supported by several findings: wood dust and leather exposure, the main etiological factors for ITAC, may cause chronic inflammation and oxidative stress resulting in the activation of NFκB, COX2 and Wnt pathway [42]. Moreover, chronic inflammation and oxidative stress generated by wood dust and leather exposure, are supposed to be responsible for the high frequency of G→A transitions inflammatory signature in TP53 and KRAS genes [2,42,43]; notably, miR-34c down--regulation has been observed in ITAC patients occupationally exposed to wood and leather [16] and it was linked to epigenetic events such as CpG island methylation or loss of transcriptional induction of p53 [44,45].

Moreover, among miR-34c gene targets, there is the Eukaryotic translation initiation factor EIF2S1 that is upregulated in ITAC [46] and that, together with EIF4B and EIF4E, is involved in mTOR pathway and Interferon type I signaling, central players in tumor-immune system interactions.

In our attempt to identify circulating biomarkers for ITAC, nasal washings were selected because of their direct contact with the tumor and not invasive collection method. MiRNA detection in nasal washings has been proposed as a diagnostic and prognostic tool for nasopharyngeal carcinoma [47] but has been never explored in ITACs. Notably, we demonstrated for the first time, that low nasal washings expression of mir-34c-3p correlates with orbital and intracranial disease extension; interestingly, miR-34c-3p is predicted to target Protein Tyrosine Phosphatase PTP4A1 and PTP4A2, two closely related family members of PTP4A3, whose gains were more frequently reported in ITACs with advanced stages and intracranial invasion [33]. Gains of PTPN1 were also more frequently associated to intracranial extension [33] and the interaction between PTPN1, also known as PTP1B, and miR-34c, experimentally demonstrated in glioma [48], has been associated with increased proliferation and metastasis in colon and lung cancer [49,50]. Since intracranial invasion and local recurrence are the most common causes of death in ITAC [39], low mir-34c levels in nasal washings appears of potential prognostic relevance in these patients. Accordingly, miR-34c-3p in serum exosomes of lung cancer patients was significantly lower than in healthy subjects and showed a negative association with disease-free survival [28]. Notably, there may be also a potential therapeutic application of mir-34c since the delivery of exosomes containing low levels of miR-34c-3p accelerated invasion and metastasis of lung cancer cells by upregulating integrin α2β1 [28]. Accordingly, in nasopharyngeal cancer cell lines, exosome containing miR-34c inhibited epithelial-mesenchymal transition and ameliorated radio resistance by targeting β-catenin/Wnt signaling [29].

Table 2
Pathways significantly enriched of genes targeted by miR-34c-3p.

Gene-Set Name	gene target of miR-34c-3p
mTOR signaling pathway:KEGG-hsa04150	AKT3|EIF4B|EIF4E|IGF1|PRKAA2
Wnt signaling pathway:KEGG-hsa04310	AXIN2|CTNNB1|LEF1|PPP2R5D| PPP3CA|PRICKLE1|PRICKLE2| SFRP1|TBL1XR1
Focal adhesion:KEGG-hsa04510	AKT3|COL6A1|CRKL|CTNNB1|FYN| IGF1|ITGA11|ITGB1|ITGB8| PDGFRA|RAP1B
Hypertrophic cardiomyopathy (HCM): KEGG-hsa05410	IGF1|ITGA11|ITGB1|ITGB8| PRKAA2|PRKAB2
Fc gamma R-mediated phagocytosis:KEGG-hsa04666	AKT3|CFL2|CRKL|MARCKS|PPAP2B| WASF2
Bacterial invasion of epithelial cells:KEGG-hsa05100	ARHGAP10|CRKL|CTNNB1|ITGB1| WASF2
Gene-Set Name	
Iron metabolism in placenta:WP2007	IREB2|SLC11A2|SLC40A1
Leptin signaling pathway:WP2034	CFL2|EIF4E|FYN|LEPR|PRKAA2|REL
Interferon type I signaling pathways:WP585	CRKL|EIF4B|EIF4E|FYN|REL
IL-1 signaling pathway:WP195	IL1A|IL1RAP|MAP3K2|PELI2|REL
Physiological and Pathological Hypertrophy of the Heart:WP1528	IL6ST|MYEF2|PPP3CA
Primary Focal Segmental Glomerulosclerosis FSGS:WP2572	CTNNB1|FYN|IRF6|ITGB1|LIMS1| SCARB2
Focal Adhesion:WP306	AKT3|CAPN1|CTNNB1|FYN|IGF1| ITGA11|ITGB1|ITGB8|PDGFRA| PELO|RAP1B
Integrin-mediated Cell Adhesion:WP185	AKT3|CAPN1|FYN|ITGA11|ITGB1| ITGB8|RAP1B
T-Cell Receptor and Co-stimulatory Signaling:WP2583	DYRK2|FYN|PPP3CA
Senescence and Autophagy in Cancer: WP615	BMI1|CD44|IGF1|IL1A|IL6ST| MDM2|RNASEL
SREBP signaling:WP1982	HMGCR|INSIG2|PRKAA2|PRKAB2| SAR1B
MAPK Signaling Pathway:WP382	AKT3|BDNF|CASP2|CRKL|IL1A| MAP3K2|PPP3CA|RAP1B|ZAK
Arrhythmogenic right ventricular cardiomyopathy (ARVC):KEGG-hsa05412:WP2118	CTNNB1|ITGA11|ITGB1|ITGB8|LEF1

Conclusion

In conclusion, the present study provides first evidence that miR-34c is detectable in nasal washings from ITAC patients showing promising associations with disease severity and extension. This is an exploratory, hypothesis generating study certainly limited by the small sample size however: 1) ITAC is a rare cancer 2) most of the studies conducted so far were retrospective other than prospective and 3) we measured miR-34c expression in different matrices such as tissues, nasal washings, and blood providing indications for further research in the field of biomarkers discovery and in the identification of potential targetable pathways involved in ITAC tumorigenesis.

Larger studies are needed to validate our results but the analysis of miR-34c in nasal washings may be considered as a potential new tool in screening and monitoring programs of ITAC patients and of professionally exposed wood and leather workers. Moreover, our findings suggest to further explore the involvement of pathways epigenetically regulated by miR-34c in ITAC tumorigenesis, for the development of new therapeutic approaches for this rare cancer.

Funding statement

This work was supported by Cassa di Risparmio di Lucca Pisa e Livorno and by the University of Florence (Fondi di Ateneo). They were not involved in the collection, analysis and interpretation of data, in the writing of the manuscript and in the decision to submit the manuscript for publication.

CRediT authorship contribution statement

Elisabetta Bigagli: Conceptualization, Investigation, Methodology, Validation, Supervision, Writing – original draft, Writing – review & editing. **Giandomenico Maggiore:** Conceptualization, Data curation, Resources, Writing – review & editing. **Lorenzo Cinci:** Data curation, Investigation, Visualization, Writing – review & editing. **Mario D'Ambrosio:** Methodology, Investigation, Writing – review & editing. **Luca Giovanni Locatello:** Data curation, Resources, Writing – review & editing. **Cosimo Nardi:** Data curation, Visualization, Writing – review & editing. **Annarita Palomba:** Data curation, Resources, Formal analysis, Writing – review & editing. **Gianluca Leopardi:** Data curation, Resources, Writing – review & editing. **Pietro Orlando:** Data curation, Resources, Writing – review & editing. **Giuseppe Licci:** Data curation, Resources, Writing – review & editing. **Oreste Gallo:** Data curation, Resources, Writing – review & editing. **Cristina Luceri:** Conceptualization, Methodology, Formal analysis, Validation, Visualization, Funding acquisition, Project administration, Supervision, Writing – review & editing.

Declaration of Competing Interest

None.

Supplementary materials

Supplementary material associated with this article can be found, in the online version, at doi:10.1016/j.tranon.2022.101507.

References

[1] I. Leivo, R. Holmila, D. Luce, T. Steiniche, M. Dictor, P. Heikkilä, K. Husgafvel-Pursiainen, H. Wolff, Occurrence of sinonasal intestinal-type adenocarcinoma and non-intestinal-type adenocarcinoma in two countries with different patterns of wood dust exposure, Cancers (Basel). 13 (20) (2021) 5245, https://doi.org/10.3390/cancers13205245. Oct 19PMID:34680393; PMCID: PMC8533857.
[2] M.A. Hermsen, C. Riobello, R. García-Marín, V.N. Cabal, L. Suárez-Fernández, F. López, J.L. Llorente, Translational genomics of sinonasal cancers, Semin. Cancer Biol. 61 (2020) 101–109, https://doi.org/10.1016/j.semcancer.2019.09.016. Apr.
[3] P. Castelnuovo, M. Turri-Zanoni, P. Battaglia, P. Antognoni, P. Bossi, D. Locatelli, Sinonasal malignancies of anterior skull base: histology-driven treatment strategies, Otolaryngol. Clin. N. Am. 49 (1) (2016) 183–200, https://doi.org/10.1016/j.otc.2015.09.012. FebPMID:26614837.
[4] D.R. Youlden, S.M. Cramb, S. Peters, S.V. Porceddu, H. Møller, L. Fritschi, P. D. Baade, International comparisons of the incidence and mortality of sinonasal cancer, Cancer Epidemiol. 37 (6) (2013) 770–779, https://doi.org/10.1016/j.canep.2013.09.014. DecEpub 2013 Oct 16. PMID:24138871.
[5] J.L. Llorente, F. López, C. Suárez, M.A. Hermsen, Sinonasal carcinoma: clinical, pathological, genetic and therapeutic advances, Nat. Rev. Clin. Oncol. 11 (8) (2014) 460–472, https://doi.org/10.1038/nrclinonc.2014.97.
[6] T.P. Robin, B.L. Jones, O.M. Gordon, A. Phan, D. Abbott, J.D. McDermott, J. A. Goddard, D. Raben, R.M. Lanning, S.D. Karam, A comprehensive comparative analysis of treatment modalities for sinonasal malignancies, Cancer 123 (16) (2017) 3040–3049, https://doi.org/10.1002/cncr.30686. Aug 15Epub 2017 Apr 3. PMID:28369832; PMCID: PMC6234843.
[7] D. Roy, A. Pascher, M.A. Juratli, J.C. Sporn, The potential of aptamer-mediated liquid biopsy for early detection of cancer, Int. J. Mol. Sci. 22 (11) (2021) 5601, https://doi.org/10.3390/ijms22115601. May 25PMID:34070509; PMCID: PMC8199038.
[8] L. Valihrach, P. Androvic, M. Kubista, Circulating miRNA analysis for cancer diagnostics and therapy, Mol. Asp. Med. 72 (2020), 100825. Aprdoi: 10.1016/j.mam.2019.10.002. Epub 2019 Oct 18. PMID:31635843.
[9] D. Roy, A. Lucci, M. Ignatiadis, S.S. Jeffrey, Cell-free circulating tumor DNA profiling in cancer management, Trends Mol. Med. 27 (10) (2021) 1014–1015, https://doi.org/10.1016/j.molmed.2021.07.001. OctEpub 2021 Jul 24. PMID: 34312074.
[10] L. Bolha, M. Ravnik-Glavač, D. Glavač, Long noncoding RNAs as biomarkers in cancer, Dis. Markers 2017 (2017), 7243968, https://doi.org/10.1155/2017/7243968. Epub 2017 May 29. PMID:28634418; PMCID: PMC5467329.
[11] E. Bigagli, L.G. Locatello, A. Di Stadio, G. Maggiore, F. Valdarnini, F. Bambi, O. Gallo, C. Luceri, Extracellular vesicles miR-210 as a potential biomarker for diagnosis and survival prediction of oral squamous cell carcinoma patients, J. Oral Pathol. Med. (2021), https://doi.org/10.1111/jop.13263. Nov 20Epub ahead of print. PMID:34800057.
[12] D.A. Clump, C.R. Pickering, H.D. Skinner, Predicting outcome in head and neck cancer: miRNAs with potentially big effects, Clin. Cancer Res. 25 (5) (2019)

1441–1442, https://doi.org/10.1158/1078-0432.CCR-18-3078. Mar 1Epub 2018 Nov 9. PMID:30413524; PMCID: PMC6415532.
[13] S.K. Gandham, M. Rao, A. Shah, M.S. Trivedi, M.M. Amiji, Combination microRNA-based cellular reprogramming with paclitaxel enhances therapeutic efficacy in a relapsed and multidrug-resistant model of epithelial ovarian cancer, Mol. Ther. Oncolytics 25 (2022) 57–68, https://doi.org/10.1016/j.omto.2022.03.005. Mar 15PMID:35399604; PMCID: PMC8971728.
[14] M.A. Cortez, D. Valdecanas, S. Niknam, H.J. Peltier, L. Diao, U. Giri, R. Komaki, G. A. Calin, D.R. Gomez, J.Y. Chang, J.V. Heymach, A.G. Bader, J.W. Welsh, *In vivo* delivery of miR-34a sensitizes lung tumors to radiation through RAD51 regulation, Mol. Ther. Nucleic Acids 4 (12) (2015) e270, https://doi.org/10.1038/mtna.2015.47. Dec 15PMID:26670277; PMCID: PMC5014539.
[15] M. Tomasetti, M. Re, F. Monaco, et al., MiR-126 in intestinal-type sinonasal adenocarcinomas: exosomal transfer of MiR-126 promotes anti-tumour responses, BMC Cancer 18 (1) (2018) 896, https://doi.org/10.1186/s12885-018-4801-z. Published 2018 Sep 17.
[16] M. Re, M. Tomasetti, F. Monaco, M. Amati, C. Rubini, G. Sollini, A. Bajraktari, F. M. Gioacchini, L. Santarelli, E. Pasquini, MiRNome analysis identifying miR-205 and miR-449a as biomarkers of disease progression in intestinal-type sinonasal adenocarcinoma, Head Neck. 44 (1) (2022) 18–33, https://doi.org/10.1002/hed.26894. JanEpub 2021 Oct 14. PMID:34647653.
[17] S. Li, X. Wei, J. He, Q. Cao, D. Du, X. Zhan, Y. Zeng, S. Yuan, L. Sun, The comprehensive landscape of miR-34a in cancer research, Cancer Metastasis Rev. (2021), https://doi.org/10.1007/s10555-021-09973-3. May 6.
[18] X. Zhou, H. Chen, L. Zhu, B. Hao, W. Zhang, J. Hua, H. Gu, W. Jin, G Zhang, Helicobacter pylori infection related long noncoding RNA (lncRNA) AF147447 inhibits gastric cancer proliferation and invasion by targeting MUC2 and up-regulating miR-34c, Oncotarget 7 (50) (2016) 82770–82782, https://doi.org/10.18632/oncotarget.13165. Dec 13PMID:27835575; PMCID: PMC5347731.
[19] C. Taverna, G. Maggiore, A. Cannavicci, P. Bonomo, M. Santucci, A. Franchi, Immunohistochemical profiling of mucins in sinonasal adenocarcinomas, Pathol. Res. Pract. 215 (7) (2019), 152439, https://doi.org/10.1016/j.prp.2019.152439. JulEpub 2019 May 4. PMID:31076280.
[20] S.H. Huang, B O'Sullivan, Overview of the 8th edition TNM classification for head and neck cancer, Curr. Treat. Opt. Oncol. 18 (7) (2017) 1–13.
[21] I. Leivo, Intestinal-type adenocarcinoma: classification, immunophenotype, molecular features and differential diagnosis, Head Neck Pathol. 11 (3) (2017) 295–300, https://doi.org/10.1007/s12105-017-0800-7. SepEpub 2017 Mar 20. PMID:28321774; PMCID: PMC5550401.
[22] H.Y. Huang, Y.C. Lin, J. Li, K.Y. Huang, S. Shrestha, H.C. Hong, Y. Tang, Y.G. Chen, C.N. Jin, Y. Yu, J.T. Xu, Y.M. Li, X.X. Cai, Z.Y. Zhou, X.H. Chen, Y.Y. Pei, L. Hu, J. J. Su, S.D. Cui, F. Wang, Y.Y. Xie, S.Y. Ding, M.F. Luo, C.H. Chou, N.W. Chang, K. W. Chen, Y.H. Cheng, X.H. Wan, W.L. Hsu, T.Y. Lee, F.X. Wei, H.D. Huang, miRTarBase 2020: updates to the experimentally validated microRNA-target interaction database, Nucleic Acids Res. 48 (D1) (2020) D148–D154, https://doi.org/10.1093/nar/gkz896. Jan 8PMID:31647101; PMCID: PMC7145596.
[23] Y.Q. Li, X.Y. Ren, Q.M. He, Y.F. Xu, X.R. Tang, Y. Sun, M.S. Zeng, T.B. Kang, N. Liu, J. Ma, MiR-34c suppresses tumor growth and metastasis in nasopharyngeal carcinoma by targeting MET, Cell Death. Dis. 6 (1) (2015) e1618, https://doi.org/10.1038/cddis.2014.582. Jan 22.
[24] K.M. Cai, X.L. Bao, X.H. Kong, W. Jinag, M.R. Mao, J.S. Chu, Y.J. Huang, X.J. Zhao, Hsa-miR-34c suppresses growth and invasion of human laryngeal carcinoma cells via targeting c-Met, Int. J. Mol. Med. 25 (4) (2010) 565–571, https://doi.org/10.3892/ijmm_00000378. AprPMID:20198305.
[25] Zhou J., Zhang B., Zhang X., Wang C., Xu Y. Identification of a 3-miRNA signature associated with the prediction of prognosis in nasopharyngeal carcinoma. Front. Oncol. 2022 Jan 27;11:823603. doi: 10.3389/fonc.2021.823603. PMID: 35155213; PMCID: PMC8828644.
[26] Y.L. Zhou, Y.J. Xu, C.W. Qiao, MiR-34c-3p suppresses the proliferation and invasion of non-small cell lung cancer (NSCLC) by inhibiting PAC1/MAPK pathway, Int. J. Clin. Exp. Pathol. 8 (6) (2015) 6312–6322. Jun 1PMID:26261507; PMCID: PMC4525841.
[27] C. Jiang, X. Zhou, Y. Zhu, Y. Mao, L. Wang, Y. Kuang, J. Su, W. Huang, S. Tang, MiR-34c-3p targets Notch2 to inhibit cell invasion and epithelial-mesenchymal transition nasopharyngeal carcinoma, Food Sci. Technol. Camp. 42 (2022) e67421.
[28] W. Huang, Y. Yan, Y. Liu, M. Lin, J. Ma, W. Zhang, J. Dai, J. Li, Q. Guo, H. Chen, B. Makabel, H. Liu, C. Su, H. Bi, J. Zhang, Exosomes with low miR-34c-3p expression promote invasion and migration of non-small cell lung cancer by upregulating integrin α2β1, Signal Transduct. Target. Ther. 5 (1) (2020) 39, https://doi.org/10.1038/s41392-020-0133-y. Apr 22PMID:32317629; PMCID: PMC7174429.
[29] F.Z. Wan, K.H. Chen, Y.C. Sun, X.C. Chen, R.B. Liang, L. Chen, X.D. Zhu, Exosomes overexpressing miR-34c inhibit malignant behavior and reverse the radioresistance of nasopharyngeal carcinoma, J. Transl. Med. 18 (1) (2020) 12, https://doi.org/10.1186/s12967-019-02203-z. Jan 8PMID:31915008; PMCID: PMC6947927.
[30] M. Re, A. Çeka, C. Rubini, L. Ferrante, A. Zizzi, F.M. Gioacchini, M. Tulli, L. Spazzafumo, S. Sellari-Franceschini, A.D. Procopio, F. Olivieri, MicroRNA-34c-5p is related to recurrence in laryngeal squamous cell carcinoma, Laryngoscope 125 (9) (2015) E306–E312, https://doi.org/10.1002/lary.25475. SepEpub 2015 Jul 7. PMID:26153151.
[31] V. Russo, A. Paciocco, A. Affinito, G. Roscigno, D. Fiore, F. Palma, M. Galasso, S. Volinia, A. Fiorelli, C.L. Esposito, S. Nuzzo, G. Inghirami, V. de Franciscis, G. Condorelli, Aptamer-miR-34c conjugate affects cell proliferation of Non-Small-Cell Lung Cancer Cells, Mol. Ther. Nucleic Acids 13 (2018) 334–346, https://doi.org/10.1016/j.omtn.2018.09.016. Dec 7Epub 2018 Sep 27. PMID:30340138; PMCID: PMC6197774.
[32] F. Palma, A. Affinito, S. Nuzzo, G. Roscigno, I. Scognamiglio, F. Ingenito, L. Martinez, M. Franzese, M. Zanfardino, A. Soricelli, A. Fiorelli, G. Condorelli, C. Quintavalle, miR-34c-3p targets CDK1 a synthetic lethality partner of KRAS in non-small cell lung cancer, Cancer Gene Ther. 28 (5) (2021) 413–426. Maydoi: 10.1038/s41417-020-00224-1Epub 2020 Sep 18PMID:32948832; PMCID: PMC8119240.
[33] J. Perez-Escuredo, A. Lopez-Hernandez, M. Costales, F. Lopez, S.P. Ares, B. Vivanco, J.L. Llorente, M.A. Hermsen, Recurrent DNA copy number alterations in intestinal-type sinonasal adenocarcinoma, Rhinology 54 (3) (2016) 278–286, https://doi.org/10.4193/Rhino15.382. SepPMID:27107016.
[34] V. Panebianco, P. Paci, M. Pecoraro, F. Conte, G. Carnicelli, Z.M. Besharat, G. Catanzaro, E. Splendiani, A. Sciarra, L. Farina, C. Catalano, E. Ferretti, Network analysis integrating microRNA expression profiling with MRI biomarkers and clinical data for prostate cancer early detection: a proof of concept study, Biomedicines 9 (10) (2021) 1470, https://doi.org/10.3390/biomedicines9101470. Oct 14PMID:34680592; PMCID: PMC8533640.
[35] K. Usuda, S. Iwai, A. Yamagata, A. Sekimura, N. Motono, M. Matoba, M. Doai, S. Yamada, Y. Ueda, K. Hirata, H. Uramoto, Relationships and qualitative evaluation between diffusion-weighted imaging and pathologic findings of resected lung cancers, Cancers (Basel). 12 (5) (2020) 1194, https://doi.org/10.3390/cancers12051194. May 8PMID:32397172; PMCID: PMC7281509.
[36] L. Martincich, V. Deantoni, I. Bertotto, S. Redana, F. Kubatzki, I. Sarotto, V. Rossi, M. Liotti, R. Ponzone, M. Aglietta, D. Regge, F. Montemurro, Correlations between diffusion-weighted imaging and breast cancer biomarkers, Eur. Radiol. 22 (7) (2012) 1519–1528. Juldoi: 10.1007/s00330-012-2403-8. Epub 2012 Mar 13. PMID:22411304.
[37] R. Stoyanova, A. Pollack, M. Takhar, C. Lynne, N. Parra, L.L. Lam, M. Alshalalfa, C. Buerki, R. Castillo, M. Jorda, H.A. Ashab, O.N. Kryvenko, S. Punnen, D. J. Parekh, M.C. Abramowitz, R.J. Gillies, E. Davicioni, N. Erho, A. Ishkanian, Association of multiparametric MRI quantitative imaging features with prostate cancer gene expression in MRI-targeted prostate biopsies, Oncotarget 7 (33) (2016) 53362–53376, https://doi.org/10.18632/oncotarget.10523. Aug 16PMID:27438142; PMCID: PMC5288193.
[38] F. Wang, Y. Wang, Y. Zhou, C. Liu, D. Liang, L. Xie, Z. Yao, J. Liu, Apparent diffusion coefficient histogram analysis for assessing tumor staging and detection of lymph node metastasis in epithelial ovarian cancer: correlation with p53 and Ki-67 expression, Mol. Imaging Biol. (2019) 21.
[39] C. Riobello, P. Sánchez-Fernández, V.N. Cabal, R. García-Marín, L. Suárez-Fernández, B. Vivanco, V. Blanco-Lorenzo, C. Álvarez Marcos, F. López, J. L. Llorente, M.A Hermsen, Aberrant signaling pathways in sinonasal intestinal-type adenocarcinoma, Cancers (Basel). 13 (19) (2021) 5022, https://doi.org/10.3390/cancers13195022. Oct 7PMID:34638506; PMCID: PMC8507674.
[40] Sánchez-Fernández P., Riobello C., Costales M., Vivanco B., Cabal V.N., García-Marín R., Suárez-Fernández L., López F., Cabanillas R., Hermsen M.A., Llorente J.L. Next-generation sequencing for identification of actionable gene mutations in intestinal-type sinonasal adenocarcinoma. Sci. Rep. 2021 Jan 26;11(1):2247. doi: 10.1038/s41598-020-80242-z. PMID: 33500480; PMCID: PMC7838394.
[41] J.P. Díaz-Molina, J.L. Llorente, B. Vivanco, P. Martínez-Camblor, M.F. Fresno, J. Pérez-Escuredo, C. Álvarez-Marcos, M.A. Hermsen, Wnt-pathway activation in intestinal-type sinonasal adenocarcinoma, Rhinology 49 (5) (2011) 593–599, https://doi.org/10.4193/Rhino.11.037. DecPMID:22125792.
[42] A. Vallée, Y. Lecarpentier, Crosstalk Between Peroxisome Proliferator-Activated Receptor Gamma and the Canonical WNT/β-Catenin Pathway in Chronic Inflammation and Oxidative Stress During Carcinogenesis, Front. Immunol. 9 (2018) 745, https://doi.org/10.3389/fimmu.2018.00745. Apr 13PMID:29706964; PMCID: PMC5908886.
[43] J. Pérez-Escuredo, J.G. Martínez, B. Vivanco, C.Á. Marcos, C. Suárez, J.L. Llorente, M.A. Hermsen, Wood dust-related mutational profile of TP53 in intestinal-type sinonasal adenocarcinoma, Hum. Pathol. 43 (11) (2012) 1894–1901, https://doi.org/10.1016/j.humpath.2012.01.016. NovEpub 2012 May 8. PMID:22575263.
[44] D.C. Corney, A. Flesken-Nikitin, A.K. Godwin, W. Wang, A.Y. Nikitin, MicroRNA-34b and MicroRNA-34c are targets of p53 and cooperate in control of cell proliferation and adhesion-independent growth, Cancer Res. 67 (18) (2007) 8433–8438, https://doi.org/10.1158/0008-5472.CAN-07-1585. Sep 15Epub 2007 Sep 6. PMID:17823410.
[45] M. Toyota, H. Suzuki, Y. Sasaki, R. Maruyama, K. Imai, Y. Shinomura, T. Tokino, Epigenetic silencing of microRNA-34b/c and B-cell translocation gene 4 is associated with CpG island methylation in colorectal cancer, Cancer Res. 68 (11) (2008) 4123–4132, https://doi.org/10.1158/0008-5472.CAN-08-0325. Jun 1PMID:18519671.
[46] Schatz C., Sprung S., Schartinger V., Codina-Martínez H., Lechner M., Hermsen M., Haybaeck J. Dysregulation of Translation Factors EIF2S1, EIF5A and EIF6 in Intestinal-Type Adenocarcinoma (ITAC). Cancers (Basel). 2021 Nov 11;13(22): 5649. doi: 10.3390/cancers13225649. PMID: 34830804; PMCID: PMC8616251.
[47] G.W. Tan, V.M. Sivanesan, F.I. Abdul Rahman, F. Hassan, H.H. Hasbullah, C.C. Ng, A.S. Khoo, L.P Tan, A novel and non-invasive approach utilising nasal washings for the detection of nasopharyngeal carcinoma, Int. J. Cancer 145 (8) (2019) 2260–2266, https://doi.org/10.1002/ijc.32173. Oct 15.
[48] Y. Shu, S. Yao, S. Cai, J. Li, L. He, J. Zou, Q. Zhang, H. Fan, L. Zhou, S. Yu, miR-34c inhibits proliferation of glioma by targeting PTP1B, Acta. Biochim. Biophys. Sin.

(Shanghai) 53 (3) (2021) 325–332, https://doi.org/10.1093/abbs/gmaa178. Mar 2PMID:33501502.

[49] S. Zhu, J.D. Bjorge, D.J. Fujita, PTP1B contributes to the oncogenic properties of colon cancer cells through Src activation, Cancer Res. 67 (21) (2007) 10129–10137, https://doi.org/10.1158/0008-5472.CAN-06-4338. Nov 1PMID: 17974954.

[50] H. Liu, Y. Wu, S. Zhu, W. Liang, Z. Wang, Y. Wang, T. Lv, Y. Yao, D. Yuan, Y. Song, PTP1B promotes cell proliferation and metastasis through activating src and ERK1/2 in non-small cell lung cancer, Cancer Lett. 359 (2) (2015) 218–225.